Photoinduced Addition of O^- to Perbromate in a Crystalline Matrix: A Pentacoordinated Bromine(VIII) Species Studied by ESR

J. R. Byberg

Department of Chemistry, Aarhus University, Langelandsgade 140, DK-8000 Aarhus C, Denmark

Received April 29, 1993®

Photolysis at 633 nm below 45 K of the radiation-produced species BrO_4^{2-} in solid $KBrO_4$ generates a paramagnetic species with a spin Hamiltonian very similar to that of the pentacoordinated species IO_5^{2-}. This strongly indicates a photoinduced transfer of O^- from BrO_4^{2-} to an adjacent BrO_4^-, where O^- becomes attached to the bromine atom to form BrO_5^{2-}, a trigonal, pentacoordinated bromine(VIII) analog of IO_5^{2-}. The formation of BrO_5^{2-} shows that the "congested" tetrahedron of BrO_4^- does not prevent the addition of a fifth ligand. In fact, rather than being governed by steric factors, the attachment of O^- to oxyanions seems linked to the ability to accommodate an excess electron, a property found in BrO_4^-, BrO_3^-, IO_3^-, and IO_4^-, which all form O^- adducts, but absent in ClO_3^- and ClO_4^-, which do not.

Introduction

In a recent paper we reported the formation of the pentacoordinated I(VIII) species IO_5^{2-} in a thermal reaction of radiation produced O^- with IO_4^- embedded in solid $KClO_4$:[1]

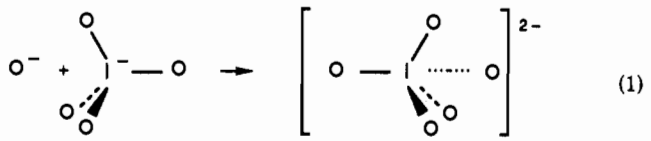

(1)

Pentacoordinated iodine species are quite common. IO_5^{2-} may in fact be regarded merely as the oxidized form of the well-characterized mesoperiodate ion IO_5^{3-},[2] and steric barriers are probably unimportant in reaction 1. In contrast to IO_4^-, BrO_4^- generally resists nucleophilic attack, presumably for steric reasons: owing to the moderate radius of the bromine atom, the tetrahedral coordination is already somewhat congested.[3] Hence addition of a fifth ligand to BrO_4^- would generate a truly supersaturated coordination, which may be expected to impede the formation of BrO_5^{2-} in a reaction analogous to reaction 1. In apparent agreement with this observation, attempts to prepare the bromine analog of IO_5^{2-} in a thermal reaction of O^- with BrO_4^- embedded in $KClO_4$ were unsuccessful. We therefore turned to a photochemical methods using X-irradiated $KBrO_4$ crystals containing the species BrO_4^{2-}, which is known to act as a source of O^-.[4] It was found that bleaching with red light below 45 K rapidly transforms BrO_4^{2-} into a new paramagnetic species with the spectroscopic properties expected for the bromine analog of IO_5^{2-}.

Experimental Section

Material and Equipment. $KBrO_4$ was synthesized by Dr. E. H. Appelman of Argonne National Laboratory. Single crystals in the form of plates measuring approximately 1 × 2 × 3 mm with the large face parallel to (001) were obtained from an aqueous solution by evaporation at room temperature.

ESR spectra were obtained with a Varian E-15 spectrometer operating at 9.3 and 35 GHz in conjunction with an AC-2-110 Cryo-Tip. Irradiation with 50-kV X-rays and subsequent bleachings at 633 nm with a 10-mW SpectraPhysics He–Ne laser were made in the microwave cavity with both kinds of irradiation incident along *c* on the same face of the sample.

Derivation of Parameters. The unit cell of the orthorhombic $KBrO_4$ crystal, containing four molecules, allows four magnetically distinct, equivalent configurations of any paramagnetic species. However, the three ESR signals described below each represents only two distinct, equivalent configurations of BrO_5^{2-}, conforming to the C_s symmetry of the anion site. Accordingly, one principal axis, *X*, of each term in the spin Hamiltonians is perpendicular to the mirror plane (*a*–*c*), so that the angular variation of the signals in this plane and the signals recorded with the static field B_0 parallel to *b* define the spin Hamiltonians completely. However, as the bromine hyperfine structure displayed by the signals is too poorly resolved to allow distinction of transitions belonging to the two abundant isotopes of bromine and, moreover, the six signals from the three pairs of equivalent configurations overlap heavily, only rather crude angular variation curves were obtained for the *a*–*c* plane. Accordingly, the **A** and **Q** tensors reported here are based primarily on computer simulations of hyperfine spectra recorded at X and Q band with B_0 parallel to the crystallographic axes, at which directions the pairs of signals from the equivalent configurations coalesce.

Results and Discussion

ESR Spectra Observed after Radiolysis. The ESR spectrum of a $KBrO_4$ crystal, recorded at 20 K after irradiation with X-rays at that temperature, consists of intense signals from the electron-excess defect BrO_4^{2-} in two inequivalent configurations, A and B, from the hole defects $(BrO_4)_2^-$ and $BrO_4 \equiv [BrO_2,O_2]$, and from trapped oxygen molecules.[5,6] Annealing at 30 K leads to the irreversible change of configuration

$$BrO_4^{2-}(B) \rightarrow BrO_4^{2-}(A) \qquad (2)$$

whereas annealing at 77 K removes $(BrO_4)_2^-$ *via* recombination with about 15% of $BrO_4^{2-}(A)$.

Photolysis of BrO_4^{2-}. Bleaching of the radiolyzed and annealed $KBrO_4$ crystal at 20 K with a 10-mW He–Ne laser leads to a rapid decay of the ESR signal from $BrO_4^{2-}(A)$ and to the emergence of signals from two new defects, arbitrarily labeled U and V, which we identify below as BrO_5^{2-} in two inequivalent configurations. In the first 10 s of the bleaching as much as 30% of $BrO_4^{2-}(A)$ may disappear. In this initial phase of the photolysis, the rates of formation of U and V, as expressed by the growth of their ESR signals, are proportional to the rate of decay of $BrO_4^{2-}(A)$ and to the amount of $BrO_4^{2-}(A)$, indicating that U and V are primary products of the photolysis of $BrO_4^{2-}(A)$.

® Abstract published in *Advance ACS Abstracts,* October 15, 1993.

(1) Byberg, J. R. *J. Phys. Chem.* **1992**, *96*, 4220.
(2) Dölling, H.; Trömel, M. *Naturwissenschaften* **1973**, *60*, 153.
(3) Downs, A. J., Adams, C. J. In *Comprehensive Inorganic Chemistry*; Trotman-Dickenson, A. F., Ed.; Pergamon Press: Oxford, U.K., 1973; Chapter 26.
(4) Byberg, J. R. *J. Chem. Phys.* **1981**, *75*, 2663.
(5) Byberg, J. R. *J. Chem. Phys.* **1971**, *55*, 4867.
(6) Bjerre, N.; Byberg, J. R. *J. Chem. Phys.* **1985**, *82*, 2206.

0020-1669/93/1332-5513$04.00/0

Table I. Parameters in the Spin Hamiltonians of BrO_5^{2-} [a]

defect	T (K)	g_x	g_y	g_z	$(\phi, \theta, \psi)^b$	A_x	A_y	A_z	$(\phi, \theta, \psi)^b$	Q_x	Q_y	Q_z	$(\phi, \theta, \psi)^b$
U	26	2.0062	2.0344	2.0010	(0, −18, 0)	36.8	7.5	27.0	(0, −13, 0)	−3.0	−0.2	3.2	(0, −70, 0)
V_u	26	2.0037	2.0185	2.0020	(0, 0, 0)	17.2	−17.0	5.5	(0, −12, 0)	−1.7	−1.8	3.5	(0, 41.5, 0)
V_s	26, 120	2.0037	2.0185	2.0020	(0, 0, 0)	16.2	−17.7	5.5	(0, −8, 0)	−1.9	−1.8	3.7	(0, 43, 0)

[a] Principal values of hyperfine and quadrupole tensors (in MHz) refer to ^{79}Br. Estimated limits of error: g_x and g_y, ±0.0005; g_z, ±0.0002; **A**, ±0.3 MHz; **Q**, ±0.2 MHz. [b] Eulerian angles, defined as in ref 7, specify the orientation of the principal axes for one of the two equivalent distinct configurations with respect to the crystallographic axes (b, a, c) of the $KBrO_4$ lattice. For the other configuration θ has opposite sign.

Table II. Reduced Hyperfine Parameters of XO_5^{2-}

species	d_x[a]	d_y	d_z	(ϕ, θ, ψ)	$10^4 a$[b]	f_x[c]	f_y	f_z	(ϕ, θ, ψ)
BrO_5^{2-}(U)	0.007	−0.009	0.002	(0, −13, 0)	7	−0.023	−0.002	0.025	(0, −70, 0)
BrO_5^{2-}(V)[d]	0.008	−0.010	0.002	(0, −10, 0)	0.5	−0.014	−0.014	0.028	(0, 42, 0)
IO_5^{2-} [e]	0.010	−0.012	0.002	(0, −19, 0)	−10	−0.009	−0.012	0.021	(0, 47, 0)

[a] Reduced dipolar hyperfine tensor $\mathbf{d} \equiv (\mathbf{A} - {}^1/_3 \text{ Tr } \mathbf{A})/a(\text{np})$ with $a(\text{np}) \equiv {}^4/_5 g_e \beta g_I \beta_I \langle r^{-3} \rangle_{nd}$ obtained from the relativistic OHFS calculations of Lindgren and Rosén:[8] (4p,Br) = 1804 MHz, a(5p,I) = 2327 MHz. [b] Reduced isotrope hyperfine constants defined as $a = {}^1/_3 \text{ Tr } \mathbf{A}/a(\text{ns})$, with the atomic hyperfine constant a(ns) taken from ref 9. [c] Relative field gradients $\mathbf{f} \equiv -2I(2I-1)\mathbf{Q}/e^2 q_{at} Q$, where $e^2 q_{at} Q$ is the quadrupole constant of the free halogen atom.[10] [d] Mean values for V_u and V_s. [e] Common arbitrary sign chosen to yield $f_z(IO_5^{2-}) \approx f_z(\text{U,V})$.

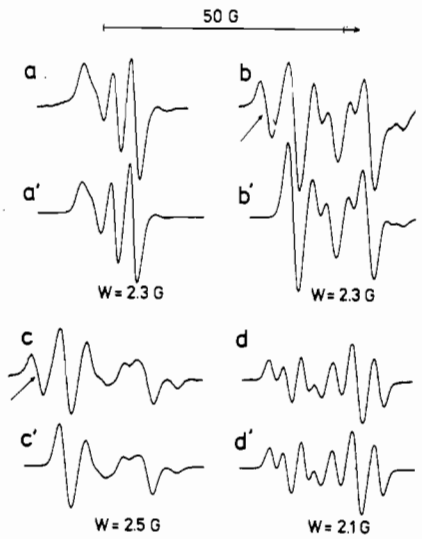

Figure 1. ESR signals from the photolytic products U (curve a), V_u (curve b), and V_s (curves c and d). B_0 is parallel to the crystallographic axis a, implying that the signals from the two equivalent configurations of each defect coalesce. Arrows indicate lines belonging to the signal from $[BrO_2,O_2]$. Curves a and b were recorded at 20 K after bleaching of the X-irradiated $KBrO_4$ crystal for 15 s (λ = 633 nm). Curves c and d were recorded at 20 and at 120 K, respectively, after bleaching for 300 s at 20 K and subsequent annealing at 77 K. For curves a–c, the microwave frequency ν_0 was 35.5 GHz; for curve d, ν_0 was 9.3 GHz. The amplitude of the 100-kHz field modulation was 0.5 G, and the nominal microwave power was 10 mW. Curves a'–d' are simulations of the observed curves, obtained with the parameters of Table I and Gaussian line shapes of width W. A significant difference between signals recorded at 35.5 and 9.3 GHz (curves c and d) demonstrates the influence of the nuclear Zeeman term.

A slight broadening and displacement of some lines in the V signal may be observed for certain directions of B_0 after prolonged bleaching, suggesting that the V signal represents two similar but inequivalent configurations in relative amounts depending on the duration of the bleaching.

At 40 K, V is the only photolytic product, and at 60 K, no photolysis is observed. At this temperature, the signal from BrO_4^{2-}(A) is unaffected by the red light, as are the signals from $[BrO_2,O_2]$ and O_2 at any temperature. The ESR signals from U and V are shown in Figure 1.

Thermal Processes. Annealing at 35 K after bleaching at 20 K leads to a fast decay of the signal from U. At 45 K, the V signal begins to decay also, attaining a constant height after annealing at 60 K. The fraction of V surviving the annealing at 60 K is stable at 120 K but decays at 140 K. Minor changes in shapes and positions of the lines, corresponding to those observed during the bleaching, accompany the partial decay of the V signal at 60 K. These observations indicate that the V signal in fact represents two paramagnetic defects V_u and V_s having very similar spin Hamiltonians but different thermal stabilities, V_u decaying below 60 K and V_s decaying at 140 K. The ratio V_s:V_u increases with increasing exposure to red light, indicating that V_s is a secondary photolytic product. Since V_s is formed also by photolysis at temperatures where V_u persists while U does not, we may assume that V_u is the precursor for V_s. The decays of the signals from U, V_u, and V_s are all accompanied by a corresponding growth of the signal from BrO_4^{2-}(A). The observed photochemical and thermal processes may be summarized as follows:

$$BrO_4^{2-}(A) \underset{\Delta\ (35\ K)}{\overset{h\nu\ (T < 35\ K)}{\rightleftarrows}} U \qquad (3)$$

$$BrO_4^{2-}(A) \underset{\Delta\ (45\text{–}60\ K)}{\overset{h\nu\ (T < 45\ K)}{\rightleftarrows}} V_u \qquad (4)$$

$$V_u \xrightarrow{h\nu\ (T < 60\ K)} V_s \qquad (5)$$

$$V_s \xrightarrow{\Delta\ (140\ K)} BrO_4^{2-}(A) \qquad (6)$$

Identification of U, V_u, and V_s. The spin Hamiltonians of U, V_u, and V_s are shown in Table I for one of the pair of equivalent configurations of each species. The hyperfine and quadrupole tensors are similar, the very small principal values indicating that the orbital containing the unpaired electron in each species has a negligible amplitude at the bromine nucleus and that the nucleus is surrounded by an almost symmetrical distribution of electronic charge. In Table II the hyperfine and quadrupole tensors are expressed in "atomic units" as the tensors **d** and **f**, respectively, for comparison with the corresponding tensors of IO_5^{2-} in $KClO_4$. With the (common) arbitrary sign chosen to yield $\mathbf{f}_z(IO_5^{2-}) \approx \mathbf{f}_z(\text{U,V})$, it appears that **d**(U) and **d**(V) are nearly identical to **d**(IO_5^{2-}), while **f**(V) resembles **f**(IO_5^{2-}). Moreover, U, V, and IO_5^{2-}all have $g_z \approx g_e$. The similarity of the spin Hamiltonian of V with that of IO_5^{2-} even extends to the orientation of the principal axes with respect to the isostructural host lattices $KBrO_4$ and $KClO_4$. On the strength of this evidence, we identify U and V as the bromine analog (BrO_5^{2-}) of IO_5^{2-} occupying two inequivalent sites. According to the discussion of

(7) Goldstein, H. *Classical Mechanics*; Addison Wesley: Cambridge, MA, 1950; p 109.
(8) Lindgren, I.; Rosén, A. *Case Stud. At. Phys.* **1974**, *4*, 197.
(9) Morton, J. R.; Preston, R. F. *J. Magn. Reson.* **1978**, *30*, 577.
(10) King, J. G.; Jaccarino, V. *Phys. Rev.* **1954**, *94*, 1610; King, J. G.; Satten, R. A.; Stroke, H. H. *Phys. Rev.* **1954**, *94*, 1798.

the bonding in IO_5^{2-} given in ref 1, this identification implies that U and V both have five Br–O bonds, one of which, however, may be weaker than the other four.

To account for the marked difference between the values of Δg_x and Δg_y for U and V, we resort to the description given in ref 1 of the electronic structure of IO_5^{2-}: The 2p orbitals on the weakly bound "odd" oxygen mix with the lone-pair 2p orbitals on the other ligands in such a way that the three occupied orbitals with highest energy are antibonding combinations, having large amplitudes ($\sim 1/\sqrt{2}$) on the odd oxygen. Consequently, matrix elements of L connecting these orbitals seem to dominate the conventional second-order representation of Δg_x and Δg_y. As the separation between the corresponding levels reflect the essentially repulsive interaction between the odd oxygen and other ligands, it follows that Δg_x and Δg_y will be sensitive to such minor structural differences as may be imposed by the inequivalent surroundings of U and V.

Mechanism of Formation and Nuclear Geometry. The identification of the product of the photolysis of BrO_4^{2-} as BrO_5^{2-} immediately suggests that the primary photolytic processes may be represented as

$$BrO_4^{2-} + BrO_4^- \xrightarrow{h\nu} BrO_3^- + BrO_5^{2-} \qquad (7)$$

i.e. as a photoinduced transfer of O^- from BrO_4^{2-} to an adjacent BrO_4^-. The spin Hamiltonians show that both configurations of BrO_5^{2-} conform to the C_s symmetry of the lattice, as does the precursor BrO_4^{2-}(A), which has a shape resembling that of BrO_4^- with two oxygens O^1 and O^2 lying in the mirror plane.[4] The observed preservation of the mirror symmetry in process 7 implies that only O^1 and O^2 can be transferred, and only to those BrO_4^- ions belonging to the mirror plane through BrO_4^{2-}(A). We propose that the configurations U and V_u result from transfer (as O^-) of O^1 and O^2 to their respective BrO_4^- neighbors along a, as shown in Figure 2. This assignment rests on the model proposed for IO_5^{2-} in $KClO_4$ and the structural similarity of this system with $BrO_5^{2-}(V_u)$, from which it follows, moreover, that the phototransferred O^- in $BrO_5^{2-}(V_u)$ becomes attached to bromine as a "normal" ligand (labeled $O^{2'}$ in Figure 2) while the original ligand O^2 becomes the odd oxygen in this configuration. By analogy, the transferred O^- in BrO_5^{2-}(U) should become the normal ligand labeled $O^{1'}$ (Figure 2), while the original ligand O^1 should become the odd oxygen. Accordingly, the addition of O^- to BrO_4^- may be considered as an "exchange process" resembling the Walden inversion

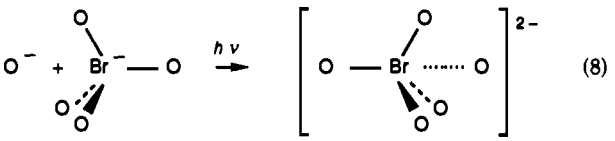

(8)

in which a normal Br–O bond is established to O^- while the bond to the oxygen sitting opposite to O^- becomes elongated. As O^1 and O^2 of BrO_4^{2-} are located near pseudo-C_3 axes of their respective BrO_4^- neighbors, the nuclear rearrangement associated with process 8 may be limited to a moderate displacement of O^1 or O^2 of BrO_4^{2-} and of the bromine atom of BrO_4^- along the pertinent C_3 axis. Hence the shape of BrO_5^{2-} should be an axially distorted, trigonal bipyramid. As discussed for IO_5^{2-} in $KClO_4$, this trigonal shape may reflect the fact that the constraints imposed by the surrounding lattice eliminate the alternative, a tetragonal pyramid. The inversion of BrO_4^- implied in process 8 probably provides the barrier preventing the immediate back-reaction that would lead to the stable configuration $BrO_4^{2-} + BrO_4^-$.

Secondary Photolysis. To account for the formation of the secondary configuration V_s, we propose that, upon excitation of V_u, O^- may move on to the next BrO_4^- along a, leaving behind an "inverted" BrO_4^- ion having a nonstandard orientation in the lattice. Figure 2 suggests that the odd oxygen O^2 of V_u, sitting near a C_3 axis of the adjacent BrO_4^-, has a position suitable for addition to this ion. The proposed exchange process is represented schematically in eq 9, and the resulting configuration ascribed to V_s is shown in Figure 2.

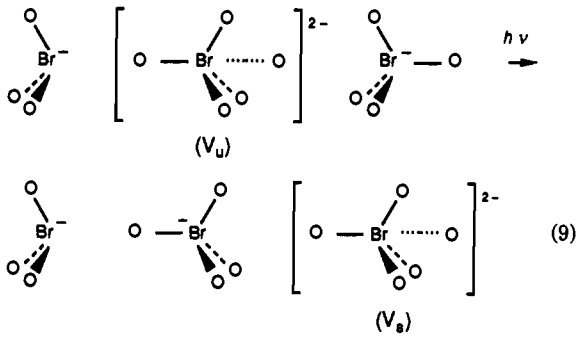

(9)

The wide separation of the thermal decays of V_s and V_u suggests that the activation energy associated with process 9 is substantially higher than that of process 8.

Correlation between O Adducts and Excess-Electron Species. In addition to BrO_4^- and IO_4^-, BrO_3^- and IO_3^- also form O^- adducts,[11,12] whereas ClO_3^- and ClO_4^- do not. Indeed, O^- sitting squeezed between ClO_3^- and ClO_4^- in solid $KClO_4$ retains its chemical identity, as reflected in the strongly anisotropic axial g tensor ($g_\perp \sim 2.05$, $g_\parallel \sim g_e$).[4]

The behavior of halates and perhalates toward radiation-produced electrons displays a similar pattern: BrO_4^-, BrO_3^-, IO_4^-, and probably also IO_3^- can accommodate an excess electron

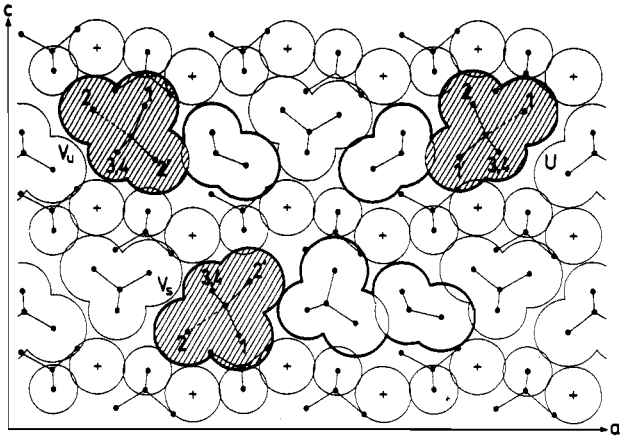

Figure 2. Structures of the primary photolytic products U and V_u and of the secondary photolytic product V_s, shown in a projection of the structure of the $KBrO_4$ crystal on the mirror plane (a–c) through the defects. Potassium ions (+) and oxygen atoms are represented as circles showing their normal effective contact radii in the mirror plane. The bromine atom of BrO_3^- has arbitrarily been given the radius of the oxygen atoms in BrO_4^-. The adducts BrO_5^{2-} are shaded, while the associated BrO_3^- and, for V_s, also the BrO_4^- with nonstandard orientation are shown in heavy lines. The atoms added as O^- to BrO_4^- are labeled $O^{1'}$ and $O^{2'}$ according to their positions in the precursor: for U and V_u, BrO_4^{2-} (not shown); for V_s, $BrO_5^{2-}(V_u)$. The assumed weak bond to the "odd" oxygen of BrO_5^{2-} is marked by a broken line. The bonds to the other oxygens, including $O^{1'}$ and $O^{2'}$, have the nominal length (1.61 Å) of BrO_4^-. O^3 and O^4 have retained their nominal positions (which seem sharply defined by the lattice geometry), while the bond angles in the mirror plane have been chosen to minimize the apparent overlap of BrO_5^{2-} with the surroundings. The same bond angles and orientations in the lattice have been adopted for V_u and V_s, in accordance with their near-identical spin Hamiltonians (Table I). The depicted configurations of U, V_u, and V_s are those that may arise from one of the two equivalent orientations of BrO_4^{2-}(A).

(11) Byberg, J. R. *J. Chem. Phys.* **1982**, *76*, 2179.
(12) Klåning, U. K.; Sehested, K.; Wolff, T. *J. Chem. Soc., Faraday Trans. 1* **1981**, *77*, 1707.

without much structural change,[4,13-15] while ClO_3^- and ClO_4^- spontaneously expel O^- upon electron capture even in solid matrices at low temperature.[4,16] It appears therefore that the ability to accommodate an excess negative charge tends to govern the formation of O^- adducts, whereas steric factors seem less important. In fact, steric considerations would indicate addition of O^- to ClO_3^- rather than to BrO_4^-, contrary to observation.

(13) Byberg, J. R., Kirkegaard, B. S. *J. Chem. Phys.* **1973**, *60*, 2594.
(14) Byberg, J. R. *J. Chem. Phys.* **1987**, *86*, 6065.
(15) Martirosyan, V. O.; Meil'man, M. L.; Marov, I. N.; Shukov, V. V. *Phys. Status Solidi B* **1975**, *68*, 791.
(16) Byberg, J. R. *J. Chem. Phys.* **1981**, *75*, 2667.